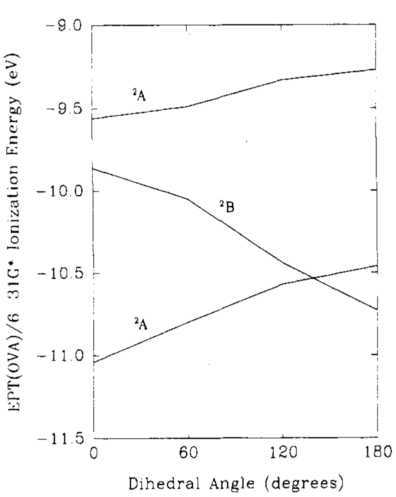

Figure 1. Electron propagator theory vertical ionization energies for tetrasilane versus dihedral angle. Labels denote final states of molecular species.

The nonadjacent Si–Si bond regions in the *a* symmetry MO's are in-phase; these regions in the *b* symmetry MO's are out-of-phase. Thus the *a* levels are destabilized and the *b* levels are stabilized as the dihedral angle increases. The ionization energies for the anti (9.27, 10.46, and 10.73 eV) and gauche (9.49, 10.05, and 10.81 eV) conformers are in close agreement with the broad experimental maxima[8] at 9.62, 10.3, and 10.85 eV. The width of each of these peaks is compatible with the concept that both conformers are contributing to the spectrum. Vertical ionization energies have a much greater conformational dependence than ground-state total energies.

Pentasilane ionization energies studied at the 3-21G* Koopmans' theorem level display similar conformation dependent trends. (Koopmans' theorem results on tetrasilane with the 3-21G* basis are not as accurate as those of Fig. 1 but give curves of similar shape.) The highest occupied MO is bonding between Si neighbors but has nodes between successive Si–Si bond regions. In going from the anti-anti to the gauche-gauche conformer, this *b* MO is stabilized by 0.35 eV because the Si_1–Si_2 and Si_3–Si_4 bond regions are in phase. The four Si–Si bonds also generate another *b* MO plus two *a* symmetry MO's. The 1–4 interaction also controls the conformational dependence of these orbital energies.[15] From these results, we infer that the highest occupied level of larger chains will consist of nearest-neighbor Si–Si bonding regions with alternating phases, as has been suggested earlier from semiempirical calculations.[12,22] The 1–4 interaction will be in phase and the energy of the level will rise as the conformation changes from gauche to anti.

In summary, our ab initio results indicate no significant difference in total energy between the anti and gauche conformers in tetrasilane and the anti-anti and gauche-gauche conformers in pentasilane when basis set and electron correlation improvements are made. Our calculated EPT vertical ionization energies are in good agreement with experimental photoelectron spectra assuming an approximately equal mix of anti and gauche rotamers. Furthermore, these results support the idea that the highest occupied MO energy level of the larger silane oligomers will decrease as the backbone is transformed from an all-anti conformation to one with a larger gauche population.

Registry No. Si_4H_{10}, 7783-29-1; Si_5H_{12}, 14868-53-2.

References and Notes

(1) For a review, see: West, R. *J. Organomet. Chem.* **1986**, *300*, 327 and references therein.
(2) Trefonas, P., III; West, R.; Miller, R. D.; Hofer, D. *J. Polym. Sci., Polym. Lett. Ed.* **1983**, *21*, 823.
(3) Zeigler, J. M.; Harrah, L. A.; Johnson, A. W. *SPIE Adv. Resist Technol. Proc. II* **1985**, *539*, 166.
(4) Harrah, L. A.; Zeigler, J. M. *J. Polym. Sci., Polym. Lett. Ed.* **1985**, *23*, 209.
(5) Miller, R. D.; Hofer, D.; Rabolt, J.; Fickes, G. N. *J. Am. Chem. Soc.* **1985**, *107*, 2172. Rabolt, J. F.; Hofer, D.; Miller, R. D.; Fickes, G. N. *Macromolecules* **1986**, *19*, 611.
(6) Trefonas, P., III; Damewood, J. R., Jr.; West, R.; Miller, R. D. *Organometallics* **1985**, *4*, 1318.
(7) Ensslin, W.; Bergmann, H.; Elbel, S. *J. Chem. Soc., Faraday Trans. 2* **1975**, *71*, 913.
(8) Bock, H.; Ensslin, W.; Fehêr, F.; Freund, R. *J. Am. Chem. Soc.* **1976**, *98*, 668.
(9) Ernst, C. A.; Allred, A. L.; Ratner, M. A. *J. Organomet. Chem.* **1979**, *178*, 119.
(10) Hummel, J. P.; Stackhouse, J.; Mislow, K. *Tetrahedron* **1977**, *33*, 1925.
(11) Damewood, J. R., Jr.; West, R. *Macromolecules* **1985**, *18*, 159.
(12) Bigelow, R. W.; McGrane, K. M. *J. Polym. Sci., Polym. Phys. Ed.* **1986**, *24*, 1233. Bigelow, R. W. *Chem. Phys. Lett.* **1986**, *126*, 63.
(13) GAUSSIAN 82, Release A by: Binkley, J. S.; Frisch, M.; Raghavachari, K.; DeFrees, D.; Schlegel, H. B.; Whiteside, R.; Fluder, E.; Seeger, R.; Pople, J. A. Carnegie Mellon University, Pittsburgh, PA.
(14) Bartlett, R. *Annu. Rev. Phys. Chem.* **1981**, *32*, 359. Binkley, J. S.; Pople, J. A. *Int. J. Quantum Chem.* **1975**, *9*, 229.
(15) Ortiz, J. V.; Mintmire, J. W. *J. Am. Chem. Soc.*, in press.
(16) Luke, B. T.; Pople, J. A.; Krogh-Jespersen, M.-B.; Apeloig, Y.; Chandrasekhar, J.; Schleyer, P. v. R. *J. Am. Chem. Soc.* **1986**, *108*, 260.
(17) See, for example: Hehre, W. J.; Radom, L.; Schleyer, P. v. R.; Pople, J. A. *Ab Initio Molecular Orbital Theory*; Wiley: New York, 1986; pp 146–164 and references therein.
(18) Pfeiffer, M.; Spangenberg, H.-J. *Z. Phys. Chem.* **1966**, *232*, 47.
(19) Öhrn, Y.; Born, G. *Adv. Quantum Chem.* **1981**, *13*, 1.
(20) Ortiz, J. V. Ph.D. Dissertation, University of Florida, Gainesville, 1981.
(21) Cederbaum, L. S.; Domcke, N.; von Niessen, W. *J. Phys. B* **1977**, *10*, 2963.
(22) Takeda, K.; Teramae, H.; Matsumoto, N. *J. Am. Chem. Soc.* **1986**, *108*, 8186.

J. W. Mintmire*
Chemistry Division, Naval Research Laboratory
Washington, D.C. 20375

J. V. Ortiz
Department of Chemistry, University of New Mexico
Albuquerque, New Mexico 87131

Received November 2, 1987

Specific Copolymerization Behavior of a Fluorocarbon Amphiphilic Macromonomer

In this paper we present a new type of macromonomer 1 and its specific behavior in copolymerization with styrene. The extremely higher copolymerizability of 1 that was assumed to be attributable to a characteristic property of the fluorocarbon chain was observed in comparison with methyl methacrylate as a model compound of 1. In contrast, a reversed trend was observable for the corre-

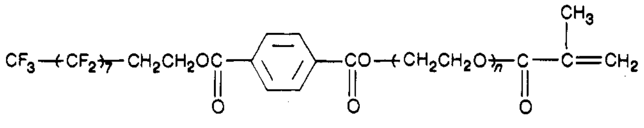

1, *n* = 10

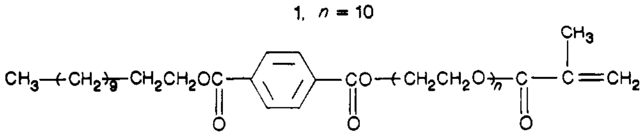

2

Scheme I

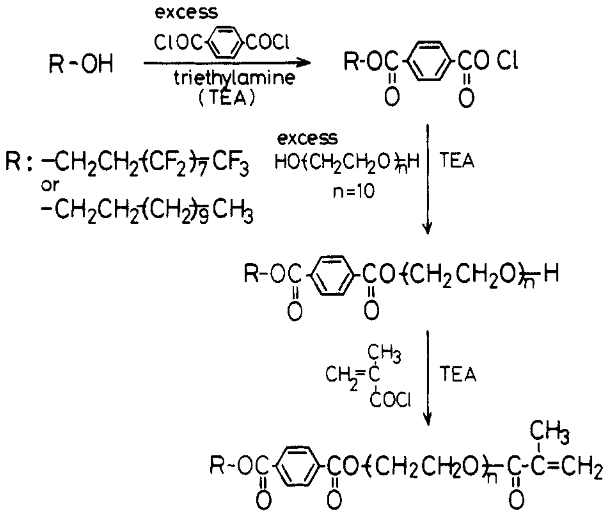

sponding hydrocarbon amphiphilic macromonomer 2–styrene copolymerization.

We have synthesized several types of macromonomers to reveal the copolymerizability with low molecular weight vinyl monomer for designing well-defined graft copolymers.[1,2] Recently, a styrene-terminated macromonomer containing a poly(oxyethylene) chain as a hydrophilic site was synthesized and it was found that the copolymerization reactivities of the macromonomer were much lower than that of a model monomer (styrene) probably due to the steric effect of the long poly(oxyethylene) chain.[3] Furthermore, the amphiphilic graft copolymer thus obtained showed a significant catalytic activity for the halogen-exchanging reaction.[3]

Ito et al.[4,5] reported on the syntheses and the copolymerization kinetics in water and organic solvents of dodecyloxy methacryloyl poly(ethylene glycol).

In this paper, we report a new type of amphiphilic macromonomer which possesses a perfluorocarbon chain and its unique copolymerizability due to a peculiar property of the fluorocarbon.

Amphiphilic fluorocarbon macromonomer 1 was prepared according to Scheme I, and the corresponding hydrocarbon macromonomer 2 was also prepared for comparison. The final products, obtained with 70–80% yield, were confirmed spectroscopically. Figure 1 shows a typical ^{1}H NMR (400 MHz with TMS as internal standard) spectrum (JOEL, JNM-GX400 FT NMR spectrometer) from a $CDCl_3$ solution of 1. Three peaks are assigned to protons of phenyl (A) (δ 8.10), vinyl (C) (δ 6.10 and 5.54), and oxyethylene (B) (δ 3.4–3.9) groups, respectively. The spectrum of 2 was similar to that of 1. The ratios of integrated intensity for each signal supported the chemical structure of 1 and 2 which possess one polymerizable methacrylate group per molecule.

Copolymerizations of 1 or 2 with styrene (St) were carried out in $CDCl_3$ with 2,2′-azobis(isobutyronitrile) (AIBN) as initiator at 80 °C. The concentration of monomers and AIBN was 2.0 and 0.02 M, respectively, and monomer composition in the feed, f_M, was set to be 0.10 in molar fraction of macromonomer. The required amounts of macromonomer, St, AIBN, and $CDCl_3$ were placed in an NMR tube and sealed after degassing, according to the conventional manner.

After polymerization, new broader peaks due to the formation of copolymers appeared in the NMR spectrum accompanying the decrease of peak intensity for vinyl protons of each monomer.

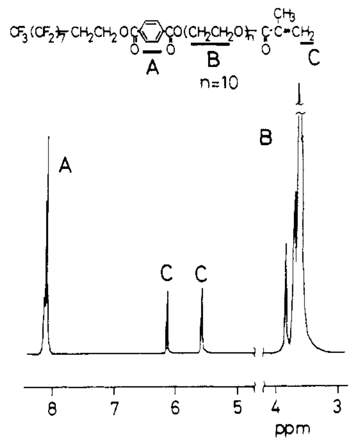

Figure 1. ^{1}H NMR spectrum for 1 in $CDCl_3$; chemical shift was measured with TMS as internal standard.

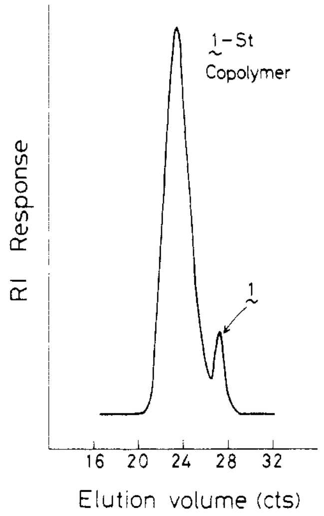

Figure 2. GPC elution pattern of 1–St copolymer with 36% conversion after purification.

Figure 2 shows a typical GPC curve of the resulting copolymer with 36% conversion purified by the reprecipitation from benzene solution into methanol to remove the unreacted monomers and the initiator. The GPC pattern supports the formation of copolymer with the number-average molecular weight $\bar{M}_n = 10\,800$, estimated by using a poly(styrene) standard. A small peak assigned to the unreacted macromonomers is, however, observable at the lower molecular weight region. In our hands, all efforts to remove the macromonomer completely by using the reprecipitation technique proved unsuccessful. Therefore, the molar fraction of macromonomer in the copolymer, F_M, and the total conversion, X_w (wt %), were estimated by making use of the amount of consumed vinyl protons. In Figure 3, cumulative copolymer composition, $\bar{F}_M$ is plotted against X_w. Interestingly, in the case of 1–St, at the lower conversion region, the values of $\bar{F}_M$ are much higher than those of f_M (0.10) and the calculated values[6] (indicated as dotted line in Figure 3) from monomer reactivity ratios ($r_{MMA} = 0.46$ and $r_{St} = 0.52$)[7] for the copolymerization of methyl methacrylate (MMA), which was employed as a low molecular weight model compound of macromonomers, and St. $\bar{F}_M$ values decrease gradually with conversion but remain higher than those of MMA–St copolymerization even at the higher conversion region. Furthermore, the pattern of the observed $\bar{F}_M$–X_w curve does not fit any theoretical curves calculated from the assumed values of monomer reactivity ratios on the basis of the integral form of the conventional copolymerization

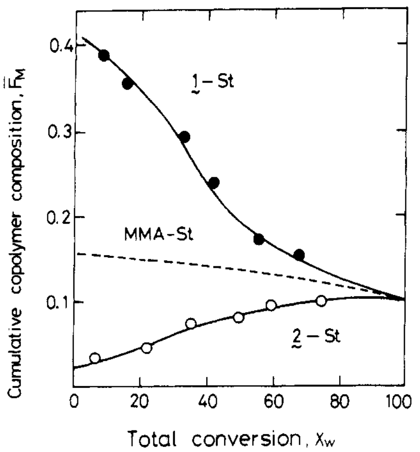

Figure 3. Relationship between cumulative copolymer composition ($\bar{F}_M$) and total conversion (X_w, wt %): black circle, 1–St; white circle, 2–St; dotted line, calculated value for the MMA–St system.

equation.[6] This deviation will not be attributable to a heterogeneity in the copolymerization system because the copolymerization reaction proceeded homogeneously up to high conversion without any precipitation. A drastic enhancement of the content of 1 incorporated in the copolymer in comparison with MMA is surprising considering the results of SOE as we reported,[3] in which the

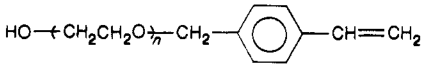

SOE, n = 46, 120

copolymerizability of SOE was much lower than that of St as a model monomer, probably reflecting the steric effect of the bulky poly(oxyethylene) chain. However, the homopolymerization of 1 proceeded much more rapidly than that of SOE up to high conversion.

On the other hand, the copolymerization profile of 2–St showed a reversed trend (as also shown in Figure 3). Copolymerizability of 2 is poorer than that of MMA in contrast to the case of 1. The difference in molecular structure between 1 and 2 exists in the hydrophobic tail which consists of a fluorocarbon-chain or a hydrocarbon-chain. Therefore, the unique behavior of 1 in its copolymerization as described above, that is, the extremely enhanced copolymerizability of 1, may be ascribable to the increase of effective macromonomer concentration as the result of formation of some aggregates and/or domains of 1 in organic solvent due to a peculiar lipophobicity of fluorocarbons.

We expect that these amphiphilic graft copolymers containing fluorocarbon chains are useful for functional applications, which are now in progress, on the basis of their aggregation states and characteristic microstructures in nonaqueous solvents.

Acknowledgment. We are grateful to T. Matsumoto for valuable technical assistance.

Registry No. 1, 113451-47-1; (1)(St) (copolymer), 113474-58-1.

References and Notes

(1) Niwa, M.; Hayashi, T.; Matsumoto, T. *J. Macromol. Sci., Chem.* **1986**, *A23*, 433.
(2) Niwa, M.; Hayashi, T.; Akahori, M. *J. Macromol. Sci., Chem.* **1987**, *A24*, 49.
(3) Niwa, M.; Akahori, M.; Nishizawa, S. *J. Macromol. Sci., Chem.*, in press.
(4) Ito, K.; Yokoyama, S.; Arakawa, F.; Yukawa, Y.; Iwashita, T.; Yamasaki, Y. *Polym. Bull.* **1986**, *16*, 337.
(5) Ito, K.; Yokoyama, S.; Arakawa, F. *Polym. Bull.* **1986**, *16*, 345.
(6) Alfrey, T.; Goldfinger, G. *J. Chem. Phys.* **1944**, *12*, 25.
(7) Brandrup, J.; Imergut, E. H. In *Polymer Handbook*; 2nd ed.; Wiley-Interscience: New York, 1975.

Masazo Niwa* and Nobuyuki Higashi
Department of Applied Chemistry
Faculty of Engineering, Doshisha University
Karasuma-Imadegawa, Kamikyo-ku, Kyoto 602, Japan

Received October 16, 1987

Estimation of the Interfacial Fraction in Partially Miscible Polymer Blends from Differential Scanning Calorimetry Measurements

During DSC studies of the partially miscible polymer blend poly[(phenylene oxide)-*co*-(sulfonylated phenylene oxide)]/polystyrene, Kang[1] found that as the sulfonylated phenylene oxide content in the copolymer is decreased toward the threshold concentration of 0.32, the ΔC_p's of the two glass transition temperatures of the blend constituents move toward each other along the temperature axis and decrease in magnitude. Fried[2] observed similar behavior in the blend poly(2,6-dimethyl-1,4-phenylene oxide)/poly(styrene-*co*-4-chlorostyrene) as the 4-chlorostyrene content of the copolymer was decreased. Fried attributed the behavior in his system to the presence of a large amount of material in the interfacial region and postulated that the amount of this material could be related to the ratio F:

$$F = \frac{w_1 \Delta C_{pu} + w_2 \Delta C_{pl}}{w_1 \Delta C_p{}^\circ{}_1 + w_2 \Delta C_p{}^\circ{}_2} \tag{1}$$

where the ΔC_{pi}'s are the step increases in heat capacity at the T_g's of the constituents before mixing, ΔC_{pu} and ΔC_{pl} are the measured increases in heat capacity at the two T_g's observed for the blend, and the w_i's are the total weight fractions of the constituents. (The ΔC_{pi}'s are assumed temperature independent). An infinitely sharp interface is therefore represented by an F-value of 1.0. While the Fried ratio may provide a qualitative measure of the extent of the actual diffuse interface in the polymer blends, it is only an approximation since the contribution of the interface is overestimated by use of the total weight fractions in the numerator of eq 1. The use of the actual weight fractions contributing to the ΔC_{pu} and ΔC_{pl} can provide an analytical expression for the amount of material in the interface, as will be shown below.

A qualitative picture of the actual interface and the resulting DSC thermogram are shown in Figure 1. The bulk regions A and B and the interface I are divided into layers of constant composition Φ_2. The T_g of each layer is a function of its composition. The ΔC_p for each layer is dependent upon the total mass in the layer. In regions of constant composition (far from the interface) such as A and B, the T_g will be fairly constant from layer to layer and therefore the ΔC_p of the layers in these regions will be additive, resulting in the two major ΔC_p's in Figure 1b.

The Couchman equation,[3]

$$\ln T_g = \frac{w_1 \Delta C_p{}^\circ{}_1 \ln T^\circ{}_{1g} + w_2 \Delta C_p{}^\circ{}_2 \ln T^\circ{}_{2g}}{w_1 \Delta C_p{}^\circ{}_1 + w_2 \Delta C_p{}^\circ{}_2} \tag{2}$$

(where $T^\circ{}_{1g}$ and $T^\circ{}_{2g}$ are the T_g's of the pure blend con-